PCCP

PAPER

Cite this: *Phys. Chem. Chem. Phys.*, 2019, **21**, 9357

Chlorine-assisted fabrication of hybrid supramolecular structures *via* electrostatic interactions†

Lei Xie, Yuanqi Ding, Xinyi Wang and Wei Xu *

Received 22nd February 2019,
Accepted 9th April 2019

DOI: 10.1039/c9cp01046g

rsc.li/pccp

Supramolecular self-assembly is a spontaneous process relying on non-covalent intermolecular interactions. Among them, electrostatic interactions generated by organic molecules interacting with alkali metals and/or halogens play an important role in structural formation. Herein, we choose cytosine and NaCl as a model system and, from the interplay of STM imaging and DFT calculations, a hybrid network composed of both metal–organic and pure organic motifs interlinked by Cl ions *via* electrostatic interactions is observed on the Au(111) surface. Moreover, the occasionally missing Cl ions in connections are accompanied by the absence of adjacent organic motifs resulting in defects of the network. This study successfully demonstrates the generality of salt providing both cations and anions simultaneously in the modulation of the structure and provides fundamental knowledge on the formation of hybrid structures as well as the function of halogens in affecting the self-assembly process.

Introduction

Supramolecular self-assembly is a process involving the spontaneous organization of various components without human intervention. It exists ubiquitously in biology[1,2] and is also well investigated in terms of bottom-up strategies for potential utilization in nanotechnology.[3,4] The principle of supramolecular chemistry is based on the synergetic effect of non-covalent intermolecular interactions[5,6] under equilibrium conditions, containing van der Waals interactions, hydrogen bonding, coordination and electrostatic interactions, *etc.* Among others, electrostatic interactions,[7] possessing non-directional and non-saturable properties, play an indispensable role in biochemistry, for instance, in the formation of G-quadruplex structures *in vivo*.[8] For on-surface investigations, supramolecular chemistry provides guidelines for the regulation of complicated structures.[9,10] Specifically, many studies have been implemented in the construction of supramolecular structures *via* electrostatic interactions.[11–19] Metal atoms, especially alkali metals, are always chosen to form metal–organic structures with molecules by bringing in electrostatic ionic bonds.[11–14] Apart from metal species, halogens with great electronegativity provide another way to regulate structures through electrostatic interactions, where halogen atoms are found to affect the molecular structures by interacting with hydrogen atoms.[15–18] As recently reported, introduction of metal halides, on the other hand, makes it possible to introduce metals and halogens simultaneously onto the surface and demonstrate an ingenious method for realizing supramolecular self-assembly modulated by various electrostatic interactions.[19] Therefore, it is of great interest to explore the generality of this facile method to obtain fundamental insight into such self-assembly processes and meanwhile detect the structural diversity in more common systems.

In this study, we choose the cytosine (C) molecule and sodium chloride (NaCl) as a model system in comparison with the previous finding about one-methyl cytosine with NaCl on the Au(111) surface.[19] The lack of a methyl group on the N1 site (see Scheme 1) greatly affects the fabrication manner of the

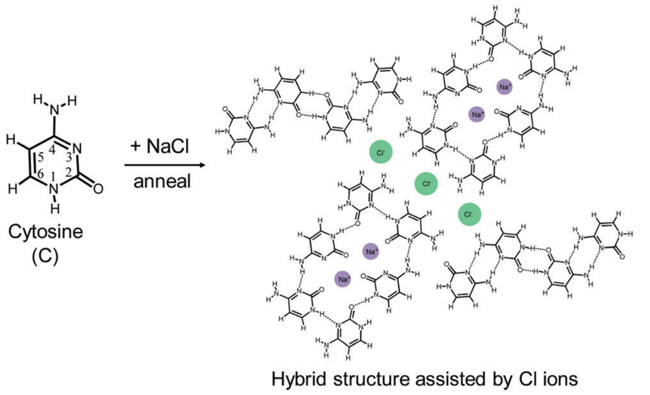

Scheme 1 Schematic illustration of the hybrid network composed of metal–organic motifs and pure organic motifs interconnected by Cl ions.

---

*Interdisciplinary Materials Research Center, College of Materials Science and Engineering, Tongji University, Shanghai 201804, P. R. China.
E-mail: xuwei@tongji.edu.cn*

† Electronic supplementary information (ESI) available. See DOI: 10.1039/c9cp01046g

whole system in an unprecedented way. From the interplay of high resolution scanning tunneling microscopy (STM) and density functional theory (DFT) calculations, we show that: (i) the generality of salt providing both cations and anions in the regulation of the structure is further demonstrated in a new and common system. (ii) The obtained ordered structure is hybrid including both metal–organic motifs and pure C molecular motifs interlinked by Cl ions as shown in Scheme 1, different from previously reported Cl ion connected pure metal–organic frameworks. (iii) Cl ions are found to link every building block of the structure together and occasionally missing Cl ions are generated along with the absence of adjacent binding motifs. This study demonstrates the generality of the strategy of salt providing both cations and anions in constructing supramolecular structures *via* electrostatic interactions. In the meantime it also provides fundamental knowledge on the fabrication of hybrid structures as well as the necessity of halogens in modulating such self-assembly processes.

Experimental and theoretical methods

All STM experiments were performed in an ultrahigh vacuum (UHV) chamber (base pressure 1×10^{-10} mbar) equipped with a variable-temperature, fast-scanning ''Aarhus-type'' STM using electrochemically etched W tips purchased from SPECS,[20,21] a molecular evaporator and other standard instrumentation for sample preparation. The Au(111) substrate was prepared by several cycles of 1.5 keV Ar+ sputtering followed by annealing at 800 K for 10 min, resulting in clean and flat terraces separated by monatomic steps. The cytosine molecules (purchased from Sigma-Aldrich, purity >99%) and NaCl (purchased from Sigma-Aldrich, purity >99%) were loaded into glass crucibles in the molecular evaporator. After a thorough degassing, the molecules were deposited onto the Au(111) substrate by thermal sublimation at 370 K and 630 K, respectively. The sample was thereafter transferred within the UHV chamber to the STM, where measurements were carried out at ~100–150 K. All the STM images were further smoothed to eliminate noise. Scanning conditions: I_t = 0.5–1.0 nA, V_t = ~1200 mV.

The calculations were performed in the framework of DFT by using the Vienna ab initio simulation package (VASP).[22,23] The projector-augmented wave method was used to describe the interaction between ions and electrons;[24,25] the Perdew–Burke–Ernzerhof generalized gradient approximation (GGA) exchange–correlation functional was employed;[26] and the dispersion-corrected DFT-D3 method of Grimme[27] was used for the calculations when including the weak interactions. The atomic structures were relaxed using the conjugate gradient algorithm scheme as implemented in the VASP code until the forces on all unconstrained atoms were ≤0.03 eV Å^{-1}.

Results and discussion

Deposition of C molecules on the Au(111) surface at room temperature (RT) results in a structure in a ''glassy state'' as shown in Fig. 1a. We can figure out that this random network is composed of interconnected C zigzag chains, which is consistent with a previous study.[28] One segment of the C zigzag chains is depicted in a blue rhomboid in Fig. 1b, which is a typical component in the self-assembled network. Note that no structural transformation is obtained after thermal treatment until total desorption as shown in Fig. S1 (ESI†).

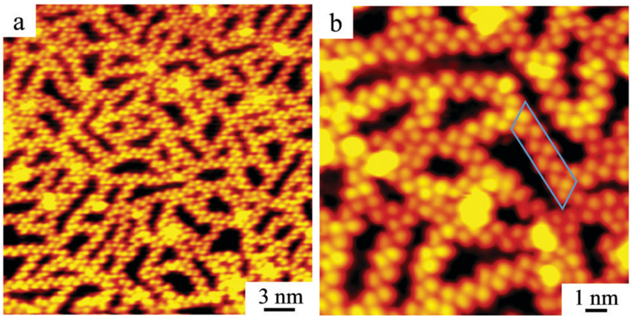

Fig. 1 (a) Large scale and (b) close-up STM images of a self-assembled C random network. The blue rhomboid highlights a typical segment of C chains where the molecules are linked in a zigzag way.

In order to study the generality of salt induced structural formation by bringing in both cations and anions, we further deposit NaCl onto the C-precovered surface. After annealing the substrate at 370 K for 10 min, an ordered porous network structure is resolved as shown in Fig. 2. From the large scale STM image (Fig. 2a), we can clearly identify that the herringbone reconstruction of the Au(111) surface remains intact, indicating weak interaction between the structure and substrate. For the purpose of distinguishing the elementary building blocks of such a structure, it is very helpful to take into consideration the arrangement at the edge of the network. As shown in Fig. 2b, the ordered structure is always ended with a motif composed of six molecules depicted in a green rectangle, which can also be found at other marginal parts and is perfectly repeatable along the long axis. As this motif has never been observed without the addition of NaCl and the integrity is also preserved in most cases, it is rational to be assigned to the metal–organic motif, which requires further analysis. Then attention has been paid to the other building block depicted in a small blue rhomboid, which resembles the segment depicted in the big blue rhomboid attached to the structure at the top left of the image, in the aspect of the zigzag binding pattern. They both exhibit great similarity with the self-assembled chain in Fig. 1b. Thus the motif is attributed to a pure organic one and composed of self-assembled C molecules. This building block can sometimes be larger as a component embedded in this hybrid structure (Fig. 2c). As a result, a partial tessellation of such an ordered hybrid network is shown in a zoom-in STM image (Fig. 2d) by blue and green contours as a guide for the eye showing the arrangement of elementary motifs.

To further reveal the structural model, we obtain a high-resolution STM image as shown in Fig. 3a. Individual molecular chiralities (depicted as R and L within two motifs) can be identified according to the morphology where the sharp end

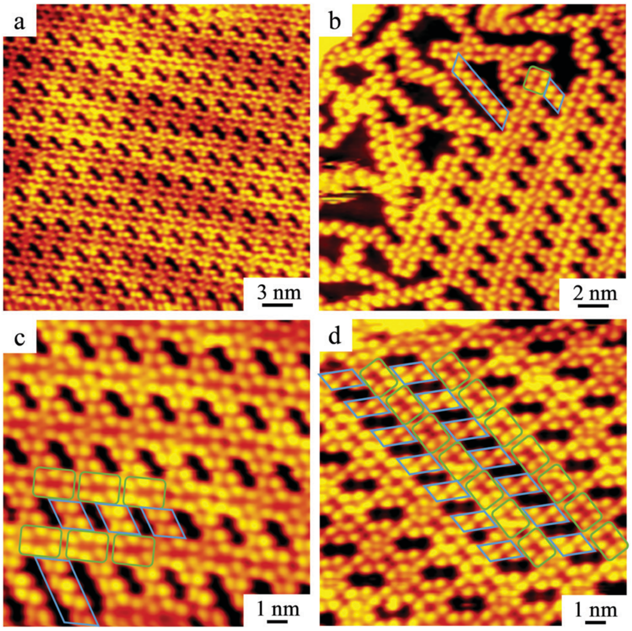

Fig. 2 Formation of the hybrid structure obtained by the addition of NaCl on the C-precovered Au(111) surface followed by further annealing at 370 K. (a) A large-scale STM image of the obtained ordered network structure. (b) The STM image taken at the edge of the network allows us to distinguish the elementary building blocks of such a structure as shown in small blue and green contours respectively. An additional large blue contour depicts a self-assembled C segment binding to the network, which resembles the small blue one in terms of the zigzag binding pattern. (c) STM image with tessellation of elementary motifs in blue and green contours in which one large blue component is also embedded in the hybrid structure. (d) STM image of an ordered network tessellated by blue and green contours as a guide for the eye showing the arrangement of the elementary motifs.

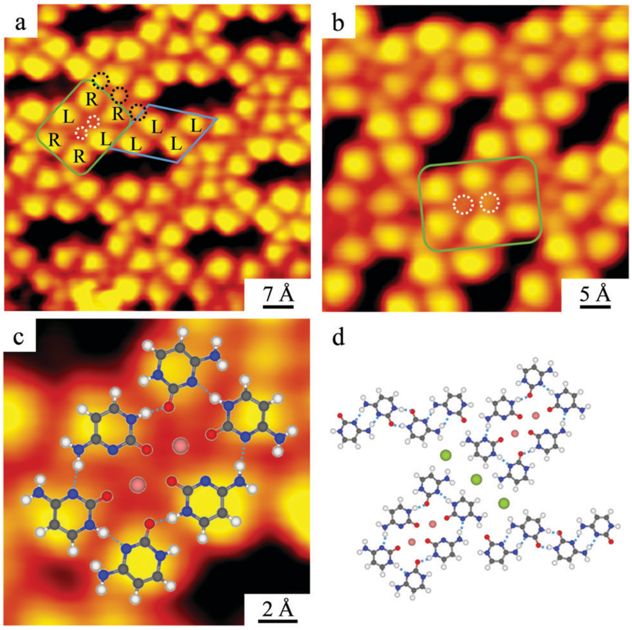

Fig. 3 (a) A high-resolution STM image helps us to identify individual molecular chiralities (depicted as R and L). The metal–organic motif is assigned to heterochiral C_6Na_2 (green contour) where the two dots within the white circles are Na ions. The pure organic motif is a homochiral C_4 cluster (blue contour). These building blocks are further linked by Cl ions depicted in black circles. (b) A high-resolution STM image taken using a special tip state where the two Na ions within the metal–organic motif in the green contour are clearly resolved as two bright dots (white dashed circles). (c) STM image superimposed with a DFT-optimized gas phase model of the C_6Na_2 motif. (d) Relaxed model showing the Cl ions connecting adjacent motifs. Hydrogen bonds are depicted as blue dashed lines. H: white; C: gray; N: blue; O: red; Na: pink; Cl: green.

of the triangle is assigned to an amino group. Detailed information about the determination of molecular chiralities is given in the Fig. S2 (ESI†). Firstly, two additional dots depicted in white circles within the metal–organic motif are observed, which can be naturally assigned to Na ions (also see a more explicit image resolving Na ions taken using a special tip state in Fig. 3b). Therefore, the heterochiral metal–organic motif in the green contour can be determined as C_6Na_2. Secondly, the motif in the blue contour can be easily assigned to a self-assembled homochiral C_4 cluster. Moreover, based on previous literature,[16,29,30] halogen atoms are always resolved as pronounced protrusions. Thus the three pronounced round dots in black circles can be assigned to Cl ions, which link every building block together forming the whole structure. It is reported that gold adatoms can only be formed by applying harsh sputtering with mild annealing,[31] thus we preclude the possibility of adatoms forming a structure on the surface. Within the metal–organic motif, Na ions interact with C molecules *via* O atoms forming ionic bonds (Fig. S3, ESI†). Among molecules NH···O and NH···N hydrogen bonds are achieved (blue dashed lines) to further stabilize the motif as shown in the DFT-optimized gas-phase model superimposed in Fig. 3c. The geometric parameters[32] for the $C{=}O\cdots Na^+$ interactions are shown in Table S1 (ESI†) where the bond length is calculated to be from 2.2 Å to 2.7 Å and the angle ranges from 106° to 173°. Moreover, the distance between two Na^+ ions is calculated to be 3.9 Å. Molecules in C_4 motifs are connected *via* double NH···O or NH···N hydrogen bonds and Cl ions serve as linkages to connect every motif by forming electrostatic interactions with the periphery hydrogen of C molecules (Fig. 3d, also see $NH\cdots Cl^-$ hydrogen bonds depicted in the enlarged image in Fig. S4, ESI†). The calculated geometric parameters for the $NH\cdots Cl^-$ interactions are shown in Table S2 (ESI†) where the bond length is calculated to be from 2.3 Å to 3.6 Å and the angle ranges from 136° to 176°. Moreover, the distance between two Cl^- ions is calculated to be 5.2 Å and 5.7 Å. Therefore, a Cl-assisted hybrid structure is fabricated by linking C_6Na_2 motifs and C_4 self-assembled motifs in an ordered way. Notably, hybrid structures of coordinated metal–organic motifs involving transition metal and pure organic motifs have been reported[29,33,34] relying on the flexibility and diversity of coordination and hydrogen bonds. The strategy presented in this system proves that electrostatic interactions are able to play a role in hybrid structural formation as well.[35]

Further analysis on the various connections composed of Cl ions linking every motif together is carried out based on high-resolution STM images in Fig. 4. In the first glance at these images, defects are observed in the porous networks and the

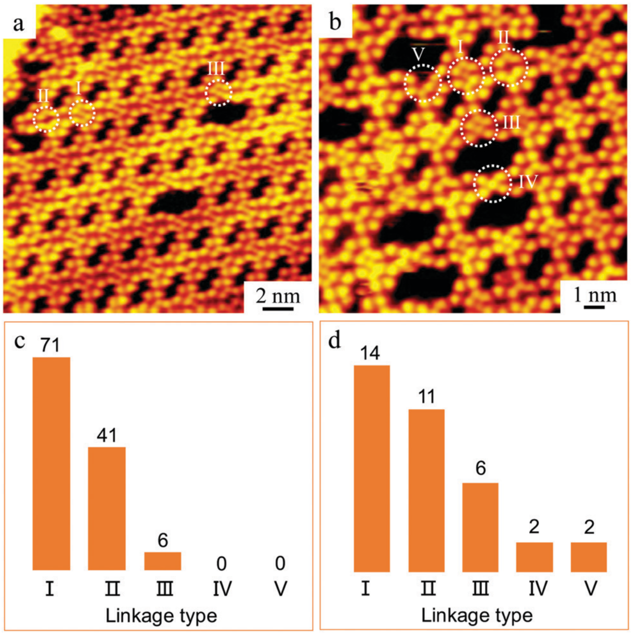

Fig. 4 Typical connections of elementary motifs formed by Cl ions are depicted in white circles. (a) An STM image with fewer defects where type I is the intact connection involving three Cl ions; type II shows the connection with the middle Cl ion missing; and type III shows the connection with one Cl ion missing at one side. (b) An STM image with more defects where type IV shows the connection with only the middle Cl ion; and type V shows the junction with only one side Cl ion. (c) and (d): distribution of the different Cl ion connections from (a) and (b) respectively.

missing motifs are always accompanied by missing Cl ions. As discussed above, there are three Cl ions lying in a linear pattern for each connection where two C_6Na_2 motifs and two C_4 segments are linked together, which can be further categorized into two kinds, namely middle and side Cl ions.

In the regular part of the hybrid network in Fig. 4a, type I and type II connections (selectively enclosed by white circles) are observed, containing all three Cl ions and both side Cl ions, respectively, which affect nothing about the regular arrangement. Interestingly, if one side Cl ion is absent (type III), the adjacent C_4 motif would be missing due to the lack of electrostatic interactions generated by the Cl ion, resulting in a defect of the structure. Fig. 4b shows the condition with more defects and some other types of connections are observed. Type IV shows the junction with only the middle Cl ion, resulting in the absence of C_4 motifs at both sides. Finally, type V shows the junction with only one side Cl ion, which also links two metal–organic motifs and the adjacent C_4 motif. The corresponding statistics about the amounts of different connection types are summarized in Fig. 4c and d, illustrating their distribution in Fig. 4a and b respectively. This bar graph gives a brief description about the degree of irregularity to some extent. It is noted that such a distribution may vary a lot in different regions of the sample and more examples are displayed in Fig. S5 (ESI†). Therefore, the electrostatic interactions formed by different Cl ions play an important role in stabilizing the whole structure.

Conclusions

In conclusion, we have successfully demonstrated the generality of the facile method of introducing salt as a supplier of both cations and anions in regulation of structures on a surface through electrostatic interactions by the combination of STM imaging and DFT calculations. Furthermore, the observed hybrid structure is composed of alkali metal–organic and pure organic self-assembled motifs interconnected by Cl ions, which is a supplement to hybrid supramolecular structures besides the ones formed by coordination bonds. The occasionally missing Cl ions are always found to disappear together with adjacent motifs, bringing in defects of the ordered network. This study offers a facile strategy in constructing hybrid structures *via* electrostatic interactions and in the meantime interprets the indispensable role of halogen ions as linkages.

Conflicts of interest

There are no conflicts to declare.

Acknowledgements

The authors acknowledge financial support from the National Natural Science Foundation of China (21622307, 21790351) and the Fundamental Research Funds for the Central Universities.

Notes and references

1 G. M. Whitesides, *Science*, 2002, **295**, 2418.
2 M. H. Robson and A. Kros, *Angew. Chem.*, 2010, **49**, 2988.
3 E. Busseron, Y. Ruff, E. Moulin and N. Giuseppone, *Nanoscale*, 2013, **5**, 7098.
4 F. P. Cometto, K. Kern and M. Lingenfelder, *ACS Nano*, 2015, **9**, 5544.
5 Y. Yang and C. Wang, *Chem. Soc. Rev.*, 2009, **38**, 2576.
6 N. Lin, S. Stepanow, M. Ruben and J. V. Barth, *Top. Curr. Chem.*, 2008, **287**, 1.
7 K. J. M. Bishop, C. E. Wilmer, S. Soh and B. A. Grzybowski, *Small*, 2009, **5**, 1600.
8 G. Biffi, D. Tannahill, J. McCafferty and S. Balasubramanian, *Nat. Chem.*, 2013, **5**, 182.
9 S. Lei, M. Surin, K. Tahara, J. Adisoejoso, R. Lazzaroni, Y. Tobe and S. De Feyter, *Nano Lett.*, 2008, **8**, 2541.
10 J. V. Barth, G. Costantini and K. Kern, *Nature*, 2005, **437**, 671.
11 D. Skomski, S. Abb and S. L. Tait, *J. Am. Chem. Soc.*, 2012, **134**, 14165.
12 C. Zhang, L. Wang, L. Xie, H. Kong, Q. Tan, L. Cai, Q. Sun and W. Xu, *ChemPhysChem*, 2015, **16**, 2099.
13 W. Xu, Q. Tan, M. Yu, Q. Sun, H. Kong, E. Lægsgaard, I. Stensgaard, J. Kjems, J. Wang, C. Wang and F. Besenbacher, *Chem. Commun.*, 2013, **49**, 7210.
14 W. Xu, J. G. Wang, M. Yu, E. Lægsgaard, I. Stensgaard, T. R. Linderoth, B. Hammer, C. Wang and F. Besenbacher, *J. Am. Chem. Soc.*, 2010, **132**, 15927.

15 T. Kaposi, S. Joshi, T. Hoh, A. Wiengarten, K. Seufert, M. Paszkiewicz, F. Klappenberger, D. Ecija, L. Đorđević, T. Marangoni, D. Bonifazi, J. V. Barth and W. Auwärter, *ACS Nano*, 2016, **10**, 7665.

16 X. Yao, L. Xie, Y. Ding, X. Wang, C. Yuan and W. Xu, *J. Phys. Chem. C*, 2018, **122**, 22959.

17 B. E. Hirsch, K. P. McDonald, B. Qiao, A. H. Flood and S. L. Tait, *ACS Nano*, 2014, **8**, 10858.

18 J. Lu, D. L. Bao, H. Dong, K. Qian, S. Zhang, J. Liu, Y. Zhang, X. Lin, S. Du, W. Hu and H. J. Gao, *J. Phys. Chem. Lett.*, 2017, **8**, 326.

19 L. Xie, C. Zhang, Y. Ding, W. E, C. Yuan and W. Xu, *Chem. Commun.*, 2017, **53**, 8767.

20 F. Besenbacher, *Rep. Prog. Phys.*, 1996, **59**, 1737.

21 E. Lægsgaard, L. Österlund, P. Thostrup, P. B. Rasmussen, I. Stensgaard and F. Besenbacher, *Rev. Sci. Instrum.*, 2001, **72**, 3537.

22 G. Kresse and J. Hafner, *Phys. Rev. B: Condens. Matter Mater. Phys.*, 1993, **48**, 13115.

23 G. Kresse and J. Furthmüller, *Phys. Rev. B: Condens. Matter Mater. Phys.*, 1996, **54**, 11169.

24 P. E. Blöchl, *Phys. Rev. B: Condens. Matter Mater. Phys.*, 1994, **50**, 17953.

25 G. Kresse and D. Joubert, *Phys. Rev. B: Condens. Matter Mater. Phys.*, 1999, **59**, 1758.

26 J. P. Perdew, K. Burke and M. Ernzerhof, *Phys. Rev. Lett.*, 1996, **77**, 3865.

27 G. Stefan, A. Jens, E. Stephan and K. Helge, *J. Chem. Phys.*, 2010, **132**, 154104.

28 R. Otero, M. Lukas, R. E. A. Kelly, W. Xu, E. Lægsgaard, I. Stensgaard, L. N. Kantorovich and F. Besenbacher, *Science*, 2008, **319**, 312.

29 L. Xie, C. Zhang, Y. Ding and W. Xu, *Angew. Chem., Int. Ed.*, 2017, **56**, 5077.

30 Q. Sun, L. Cai, H. Ma, C. Yuan and W. Xu, *ACS Nano*, 2016, **10**, 7023.

31 C. Chen, H. Sang and P. Ding, *et al.*, *J. Am. Chem. Soc.*, 2018, **140**, 54.

32 M. Ghorbanpour, M. P. Wemhoff, P. Kofoed and R. D. Parra, *J. Undergrad. Chem. Res.*, 2007, **6**, 135.

33 H. Kong, C. Zhang, L. Xie, L. Wang and W. Xu, *Angew. Chem., Int. Ed.*, 2016, **55**, 7157.

34 H. Kong, C. Zhang, Q. Sun, X. Yu, L. Xie, L. Wang, L. Li, S. Hu, H. Ju, Y. He, J. Zhu and W. Xu, *ACS Nano*, 2018, **12**, 9033.

35 D. Peyrot and F. Silly, *J. Phys. Chem. C*, 2017, **121**, 20986.